

On the Properties of Dielectric Elastomer Actuators and Its Implications for Their Design

J.-S. Plante and S. Dubowsky
Massachusetts Institute of Technology, Room 3-469, 77 Mass. Ave,
Cambridge, MA, 02139

E-mail: jsplante@mit.edu

Abstract. Dielectric Elastomer Actuators (DEA) have been studied extensively under laboratory conditions where they have shown promising performance. However, in practical applications, they have not achieved their full potential. Here the results of detailed analytical and experimental studies of the failure modes and performance boundaries of DEAs are codified into design principles for these actuators. Analysis shows that the performance of DEAs made with highly viscoelastic is governed by four key mechanisms: pull-in failure, dielectric strength failure, viscoelasticity and current leakage. A design map showing the effect of these four mechanisms on performance under varying working conditions is proposed. This study shows that the viscous nature of DEA is very important in their performance/reliability trade-offs. A proper balance of performance and reliability is key to successful design of DEAs.

Keywords: Dielectric, Elastomer, Design, Failure, Performance

1. Introduction

Dielectric Elastomer Actuators (DEA) have been proposed as a potentially important component for robotic and mechatronic devices. These actuators have shown good laboratory performance and are inexpensive [1,2]. They are lightweight, simple, have large displacements and good force capabilities

[3,4,5,6,7]. Possible applications of DEAs vary from medical devices to space robotics [8,9,10,11]. Fig. 1 shows a diamond actuator with its frames and actuating films as well as a prototype performing extension strains of 100%.

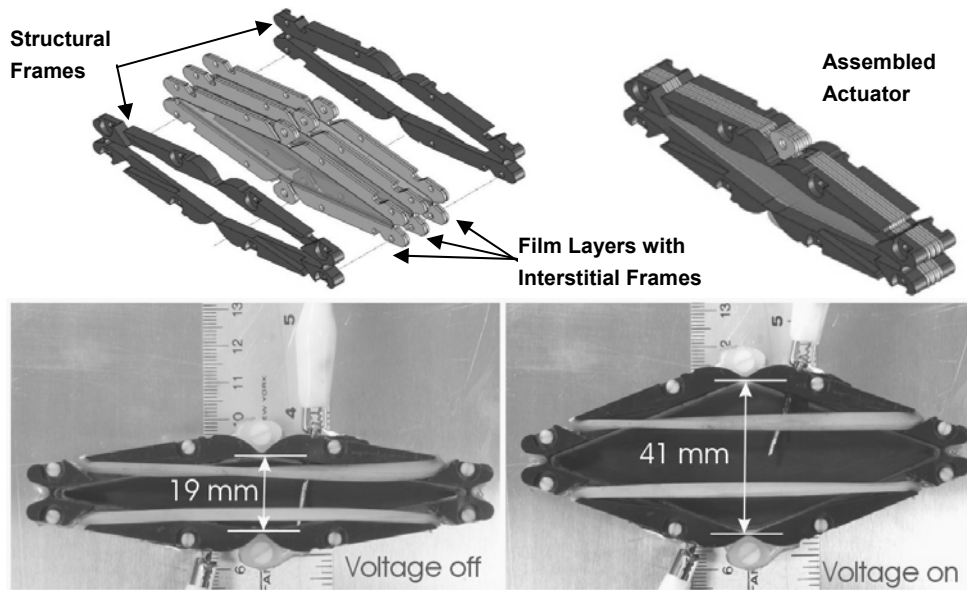


Fig. 1: Assembly and prototype of diamond shaped actuators.

Early assessments of ideal DEA performance based on 3M’s VHB 4905/4910 elastomer films, a common material used in DEAs, suggested extensions of up to 3 times their initial length [5], bulk material force-to-weight ratio of 1000:1 [5], and bulk material specific energy densities of 3-4 J/g [4]. However, experiments have shown “infant mortalities”¹ of about 30%, shelf lives of a few weeks, and most importantly, erratic and not well understood failures during operation [10,11]. DEAs have generally been pictured as being elastic materials with excellent (almost perfect) electrical isolation properties. This conceptual representation does not anticipate the above problems. This suggests that the fundamental mechanisms of DEAs behavior were not completely understood. This paper explains how the key performance mechanisms and failure modes of DEAs influence their design space.

¹ Immediate failure upon first voltage application.

1.1. Background

The majority of DEA research have explored new actuator shapes and potential applications [4,5,6,7,10,11,12,13,14,15,16,17]. Some models of the mechanics of DEA behavior have been proposed. In particular, a failure mode called *pull-in*² has been studied. Various modeling approaches were use such as linear (Hookean) models [18,19,20] and hyper-elastic continuum mechanics ones [24]. These studies explained the basics of pull-in failure but did not explain the erratic failures encountered in practical actuators.

Viscoelasticity is another mechanism that plays a significant role in the performance of DEAs. Frequency response experiments of DEAs have shown significant displacement attenuation with increasing frequency or stretch rate, with up to 90% attenuation at 10Hz [21,22]. Viscoelastic models have been developed for DEA materials [23,24,25]. However, their application to the quantitative analysis of viscoelasticity's role in DEAs performance under load has not been done.

Another important physical mechanism affecting DEAs performance is electrical current leaking through the film. These currents have an important impact on actuator efficiency. Their presence have only been briefly considered in past researches [10,11,18,19].

1.2. Objective

Recent fundamental studies have made important progress in understanding the failure modes and performance limits of DEAs [26,27,28]. The objective of this paper is to first review these results and then show how they influence the design of DEAs. It is shown here that four key properties, pull-in failure, dielectric strength failure, viscoelasticity, and current leakage, govern the design of DEAs. The conditions leading to failures of DEAs (material strength, dielectric strength, and pull-in) have been identified [27]. Analytical model results shows that practical actuators operating under work loads have failure modes that varies depending on stretch rate. At high stretch rates, dielectric strength is the dominant mode of failure and large extensions are possible. At low stretch rates, pull-in is the dominant mode of failure and limits extension

to low values. Experimental studies have shown that viscoelasticity and current leakage are the governing mechanisms for power and efficiency [28].

In this paper, the effect of these four key properties on DEA design and operation is discussed. A map of the design space is proposed that quantitatively highlights the most relevant performance and reliability trade-offs of DEAs. Possible applications of DEAs are proposed and their performance is compared to conventional voice coil actuators.

2. Failure modes

Here an analytical model of DEA is presented (for more details, see references [26,27]). Failure criteria are formulated and the model is used to predict failure under various conditions of speeds and working loads. Predictions are compared with experimental results. The analysis does not include localized effects such as voids, inclusions, mechanical stress concentration, electric field concentration, and time dependant failures such as creep or fatigue [10,26].

2.1. Analytical model

Consider the system of a small conductive circle coated in the center of a large pre-stretched film as shown in Fig. 2. Under Maxwell pressure, the expanding circle's radius increases from its pre-stretched value, r_{pre} , to its actuated value, r_{act} . The film deformation of such devices occurs far away from the film's rigid ring ($r_{rig} > r_{act}$) and local failures due to the film bonding interface are minimized, putting emphasis on fundamental basic material failure modes. However, these devices are not actuators because they cannot provide external working loads. The effect of actuator load is considered by imposing an artificial loading stress.

² A pull-in failure occurs when the Maxwell pressure becomes greater than the film's compressive stress. This leads to an unstable compression of the elastomer material and catastrophic failure ultimately caused by a dielectric strength or material strength failure.

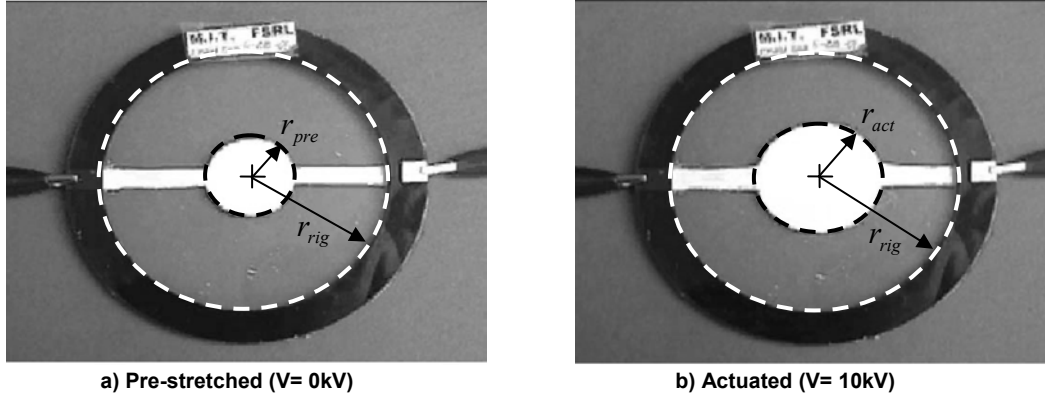


Fig. 2: Expanding circle.

The film is modeled as a hyper-elastic material. The viscoelasticity is modeled by defining different elastic material models at different stretch rates. Hence, all deformations are assumed to occur at constant stretch rates. This strategy is more tractable and reliable than models where stretch rate is a variable.

The deformation of the active region (expanding circle) is illustrated in Fig. 3. The deformation is decomposed into two consecutive deformations: the pre-stretch deformation required to avoid film buckling and the actuation deformation. The dimensions in the reference configuration (prior to pre-stretch) are expressed in the R, Θ, Z system. The dimensions in the pre-stretched and actuated dimensions are expressed in the r, θ, z coordinates. The pre-stretch deformation is due to the stretching of the film prior to actuation. It consists of imposed biaxial or equibiaxial deformations that produce principal stresses³ in the pre-stretched configuration, $\sigma_{1,pre}, \sigma_{2,pre}, \sigma_{3,pre}$. The pre-stretched configuration is then perturbed by the equivalent Maxwell pressure, P , resulting from voltage application. The film further deforms and the stresses in the actuated configuration reach a new equilibrium to $\sigma_{1,act}, \sigma_{2,act}, \sigma_{3,act}$.

The Maxwell stresses are expressed by an equivalent Maxwell pressure, P , given in references [19,34]:

$$P = -\varepsilon_d \varepsilon_0 \left(\frac{V}{u_{act}} \right)^2 \quad (1)$$

³ The stresses are “true” stresses or Cauchy stresses and are expressed in the deformed configuration: $\sigma = F/A_{deformed}$.

where ε_0 is the free-space permittivity (8.85×10^{-12} F/m), ε_d is the material's dielectric constant, V is the voltage applied across the electrodes, and u_{act} is the actuated film thickness.

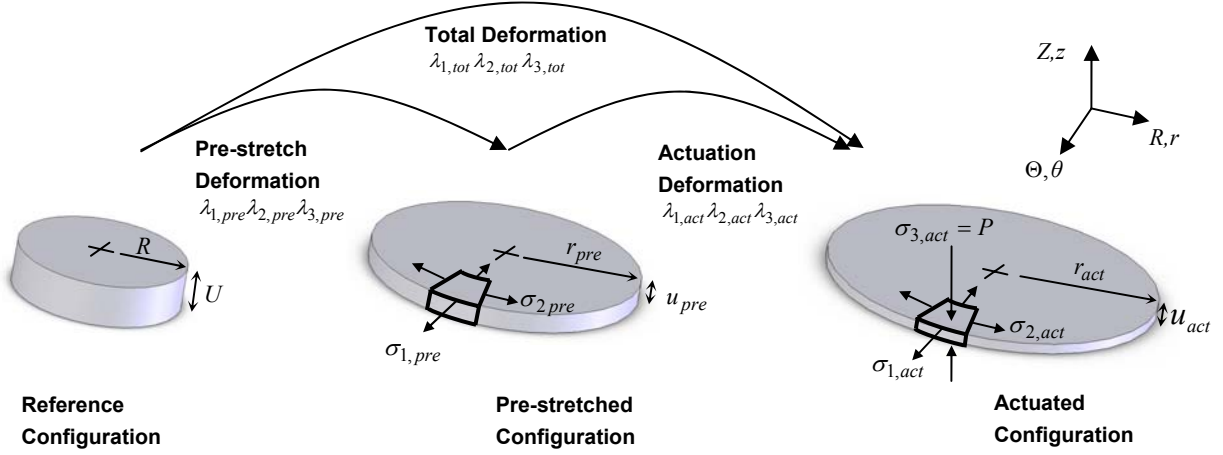


Fig. 3: The deformations and stresses of the active region.

The objective of the model is to find the actuation stretches, $\lambda_{i,act}$, for any given voltage, V , mechanical pre-stretch, $\lambda_{i,pre}$, stretch rate of the uniaxial test used to define the elastomer constitutive model, $\dot{\lambda}_{UNI}$, and working load, σ_{load} :

$$\lambda_{i,act} = f(V, \lambda_{i,pre}, \dot{\lambda}_{UNI}, \sigma_{load}) \quad i = 1, 2, 3 \quad (2)$$

The actuation stretch, $\lambda_{1,act}$, is reached when the equivalent Maxwell pressure, P , of Eq. (1) is in equilibrium with the film's axial stress:

$$P(V, \lambda_{1,pre}, \lambda_{1,act}) = \sigma_{3,act}(\lambda_{1,pre}, \lambda_{1,act}, \sigma_{load}) \quad (3)$$

The axial stress, $\sigma_{3,act}$, is found from a stress/stretch model based on Ogden's formulation [29,30] given by:

$$\sigma_{3,act} = \sigma_{1,act} - \mu_1 (\lambda_{1,tot})^{\alpha_1} - \mu_2 (\lambda_{1,tot})^{\alpha_2} + \mu_1 (\lambda_{3,tot})^{\alpha_1} + \mu_2 (\lambda_{3,tot})^{\alpha_2} \quad (4)$$

The film planar stress, $\sigma_{1,act}$, of Eq. (4) has two components: 1) the stress due to the deformation of the film's passive region, $\sigma_{passive\ region}$, and 2), the stress of the working load, σ_{load} , such that:

$\sigma_{1,act} = \sigma_{passive\ region} - \sigma_{load}$. The passive region stress is found from an elaborate finite difference model beyond the scope of this paper [26,27]. The load stress is estimated from practical diamond actuators as shown in Fig. 1. The parameters used in this paper are: a single 1.5 mm layer of 3M's VHB 4905/4910 elastomer, pre-stretches of $\lambda_{1,pre} \times \lambda_{2,pre} = 5 \times 2.2$ for a pre-stretched area expansion of 11, a closed diamond major axis of 107 mm, an operating voltage of 10 kV, and maximum linear strains of 150%. Many polymer film materials were studied in the past 10 years. The material giving the best performance is 3M's VHB 4905/4910 [18,31,32,33,34,35,36,37,38,39]. Hence, this paper focuses on VHB 4905/4910. The load stress is given by the following empirical relation (units of MPa) [26]:

$$\sigma_{load} = [0.14 + 0.56(\lambda_{1,act} - 1)] \Delta F \quad (5)$$

where $\Delta F \sim 1.75$ N at low stretch rates ($\dot{\lambda}_{UNI} = 3.3 \times 10^{-4} \text{ s}^{-1}$) and ~ 0.875 N at high stretch rates ($\dot{\lambda}_{UNI} = 0.094 \text{ s}^{-1}$). ΔF is the mean force difference between the ON and OFF curves of a complete actuation cycle (as shown later in Fig. 7).

2.2. Failure criteria:

2.2.1. Material strength failure: It is assumed that material strength failure occurs when folded polymer chains are straightened beyond their unfolded length. This kind of failure is thus primarily a function of stretch. Failure takes place when the film area expansion is higher than the film's experimentally determined limit of 36 [23,40]:

$$\lambda_{1,tot}^2 > 36 \quad (6)$$

2.2.2. Dielectric strength failure: Dielectric failure is predicted from an empirical breakdown voltage vs. total stretch curve obtained for rigid (non-deforming) electrodes. The maximum actuation stretch is obtained when the model's electric field is higher than the experimental dielectric strength:

$$E > E_{EXP}(\lambda_{1,tot}) \quad (7)$$

2.2.3. *Pull-in instability failure:* Pull-in instability appears when the equilibrium condition of Eq. (3) cannot be reached and the film collapses into highly complex 3D wrinkling patterns leading to failure from either dielectric or material breakdown. A simplified one-dimensional model capable of predicting the onset of pull-in instability is found by analyzing the equilibrium between the opposing stresses, P and $\sigma_{3,act}$, obtained respectively from Eqs. (1) and (4). The ultimate actuation stretch before pull-in is at the last stable intersection between the Maxwell pressure, P , and the film's axial stress, $\sigma_{3,act}$.

2.3. Model predictions and experimental verification

The above model and failure criteria were used to predict the failure of expanding circles for various film pre-stretches, at low and high stretch rates with working loads. Predictions were made for two different stretch rates, respectively called low and high stretch rates and corresponding to $\dot{\lambda}_{UNI}=3.3 \times 10^{-4} \text{ s}^{-1}$ and 0.094 s^{-1} . The high stretch rate of $\dot{\lambda}_{UNI}=0.094 \text{ s}^{-1}$ is typical of many DEA applications, while the low stretch rate of $\dot{\lambda}_{UNI}=3.3 \times 10^{-4} \text{ s}^{-1}$ is the equilibrium rate where viscoelastic effects are negligible.

Analytical model predictions are compared with experimental data of 10 identical diamond actuators (see Fig. 1). The samples were first tested at high stretch rates, with no failures. The same samples were then tested at low stretch rates and all 10 failed. The data is presented in Fig. 4. The average linear strain at failure was 30% (or equivalently, an area expansion of 1.28) with a lowest value of 6% (or equivalently, an area expansion of 1.05). The predictions corroborate well with the data. The figure also show that a pre-stretch area expansion of about 11 is optimum for actuators operating at high stretch rates.

The differences between low- and high- stretch rate failure predictions show the fundamental role of viscoelasticity on actuator failure. Viscoelasticity significantly affects the amount of viscous impedance at high stretch rates. These viscous forces “stiffen” the film and protect it from pull-in failures, with dielectric strength governing failure. In contrast, low stretch rates generate less viscous impedance and pull-in failures dominate.

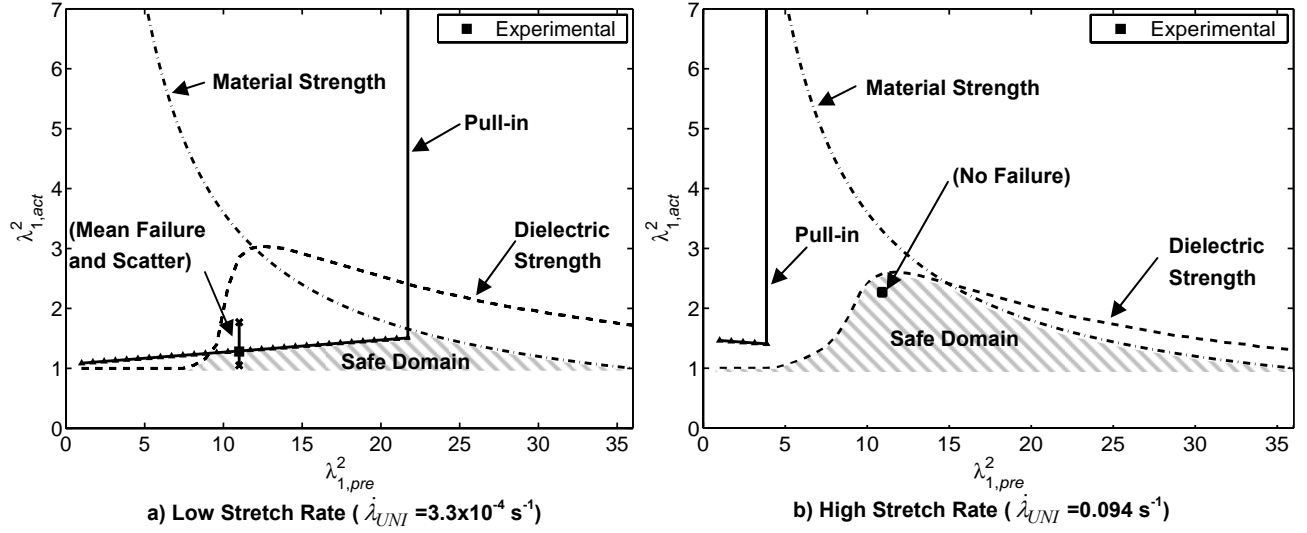


Fig. 4: Failure analytical predictions for low and high stretch rate with loading stress.

3. Performance of DEAs

The performance of diamond actuators (see Fig. 1) was studied over a range of actuation velocities and strokes in a test called *work cycle*. These cycles consisted of opening and closing actuators under imposed, constant, velocities [26]. In these tests, the elastic bands used to preload the film are not used since these conservative elements (in first approximation) have no net work production over a complete cycle. A 10 kV voltage was applied during actuator opening only. Actuator force and current were measured during actuator opening and closing.

3.1. Experimental observations

The measured force/stroke profiles lead to the actuator work output map shown in Fig. 5. The work output is the mechanical energy outputted for a given cycle and is defined by the closed integral of actuator force, F , on actuator stroke, ds :

$$W_O = \oint_{cycle} F ds \quad (8)$$

As shown in Fig. 5, maximum work output is located at the lowest speed (low stretch rates) and highest extensions. These conditions lie exactly in the pull-in failure domain. Hence, optimal work output

performance cannot be obtained without sacrificing actuator life, and the design of DEAs therefore implies fundamental reliability/performance trade-offs.

An actuator efficiency map is shown in Fig. 6. Actuator cycle efficiency is defined by the ratio of the cycle's energy output over its energy input:

$$\eta = \frac{W_O}{W_I} \quad (9)$$

The energy output, W_O , is Eq. (8). The energy input, W_I , must account, not only for the supplied electrical energy, but also for the mechanical energy supplied by the testing apparatus to fight the viscous impedance in order to maintain constant velocities:

$$W_I = \oint V i dt + \oint \Delta F_V ds \quad (10)$$

where V is the voltage, i is the current, and ΔF_V is the viscous impedance force. The viscous impedance force is estimated by comparing force measurements against the equilibrium value taken at very low velocity where viscous forces are negligible.

The efficiency map of Fig. 6 appears like a folded curtain and present a peak of about 12 %. The figure shows clearly the fundamental effects of viscoelasticity and current leakage. At high speeds, efficiency is limited by viscoelasticity (under these test conditions). At low speeds, efficiency is limited to small values ($\eta \ll 1\%$) because of important current leakage through the film. Models validating these two mechanisms were developed and are briefly explained bellow.

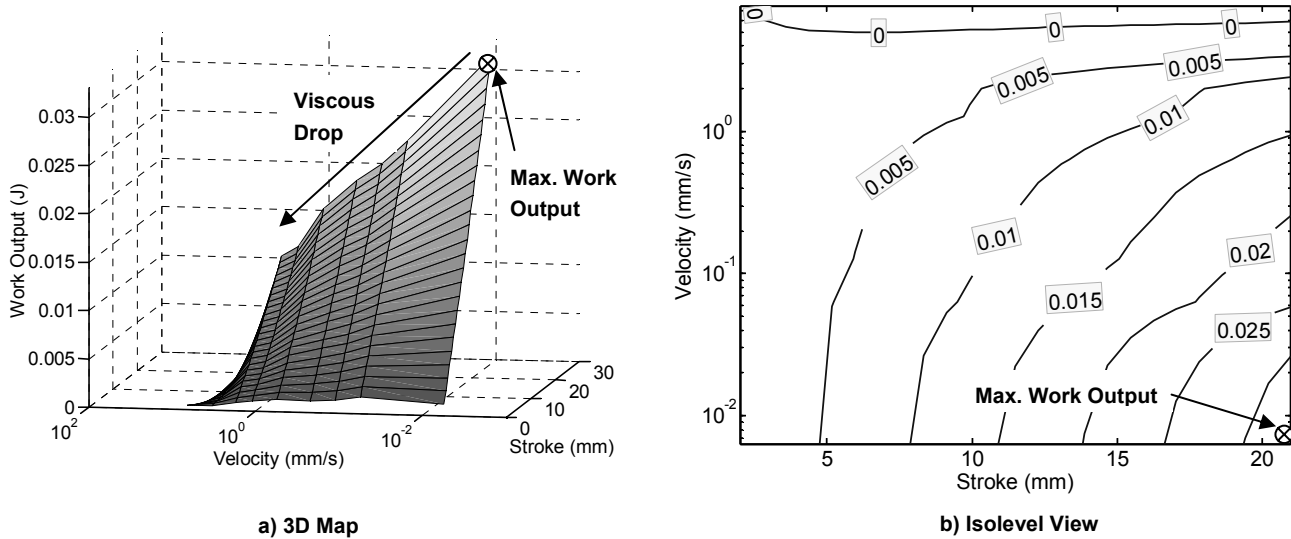


Fig. 5: Cycle work output map.

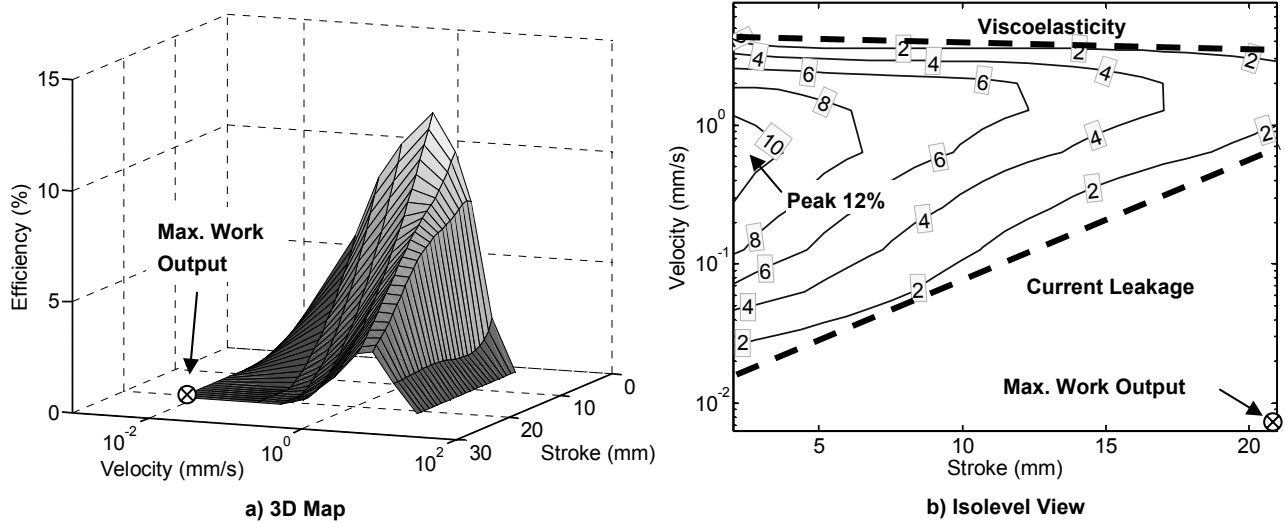


Fig. 6: Efficiency map.

3.2. Viscoelastic model:

A viscoelastic model based on the Bergstrom-Boyce formulation was developed and showed excellent agreement with experimental data [26,28]. For example, Fig. 7, shows a comparison of model predictions and experimental force/stroke profiles at two different velocities. The ON curve corresponds to actuator opening with voltage applied and the OFF curve is the return without voltage. The model shows how the force difference, ΔF , attenuates as velocity increases due to viscous impedance.

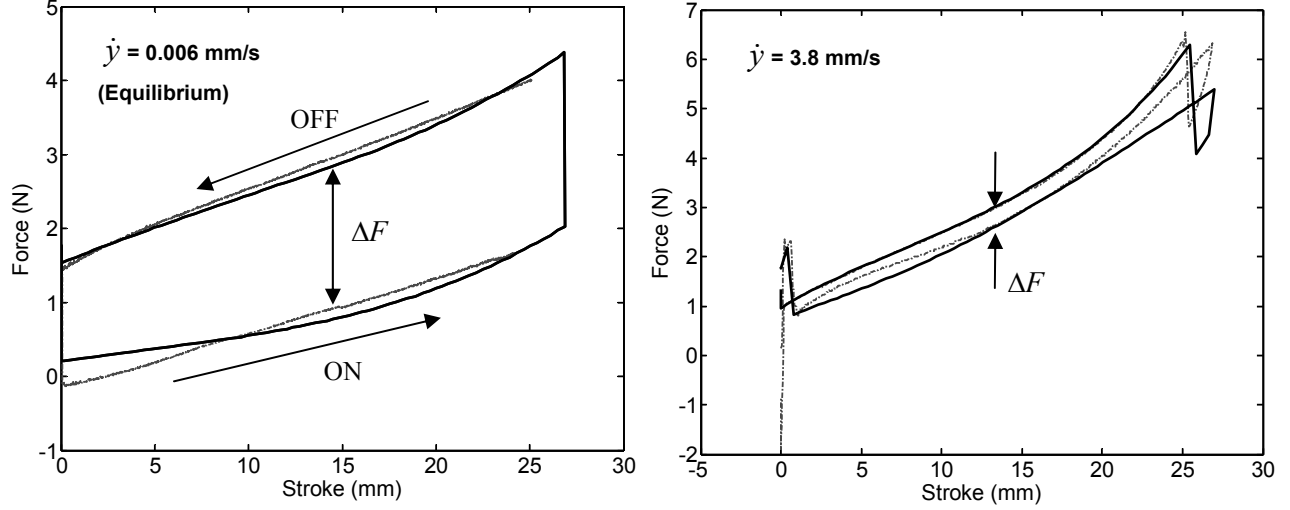


Fig. 7: Viscoelastic model, prediction (dark) vs. experiment (light).

3.3. Current leakage model

A first order model of current leakage that includes a conductive and a diffusive leakage term has been developed [26,28]. Conductive leakage considers the film as a classical conductor with a fixed bulk resistivity, ρ . Diffusive leakage considers that the film's resistivity is locally doped by the migration of charges into the polymer from the film's surface [41]. The diffusion current is given by:

$$i(t) = K \frac{\left(1 - \operatorname{erf}\left(\frac{u}{2\sqrt{\alpha t}}\right)\right)}{u^2} V \quad (11)$$

where, u is the instant film thickness, t is the time, V the voltage, α the diffusion constant and K a constant. Model predictions compared to experimental data is shown in Fig. 8. Both the model and experimental data shows the characteristics of diffusive processes where the quantity of interest varies not only in space but also in time such as heat diffusion and boundary layers. Hence large current consumption is not only observed at large extension, but also at low speeds. The molecular nature of the proposed diffusive leakage requires further studies. Possible impacts of current leakage on film properties and its coupling with failure modes is unknown.

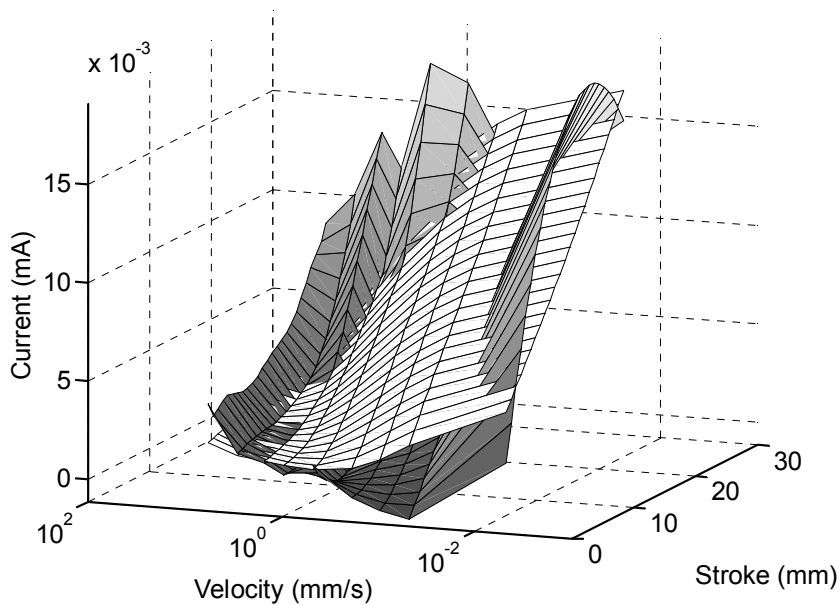


Fig. 8: Current leakage model predictions (white) vs. experiments (grey).

4. Implications on design and operation

4.1. Design space

The failure and performance study results are combined to map the design space of DEAs based on VHB 4905/4910 material and pre-stretched optimally to an area expansions of about 11, see Fig. 9. These maps are given in non-dimensional terms of actuation stretch and stretch rates. Care should be taken in using the numerical values of these maps because: 1) they are based on limited data, 2) they contain no safety factor, and 3) they were obtained for diamond actuators and may not correspond perfectly to other designs.

Fig. 9a and b highlight the fundamental reliability/performance trade-off caused by viscoelasticity. Fig. 9a shows that actuator output force decreases under viscoelastic impedance as velocity increase. At stretch rates above $\sim 5 \times 10^{-4} \text{ s}^{-1}$, viscoelasticity reduces practical forces and stretches to very small values. Fig. 9b shows that, at low stretch rates, below $\sim 3 \times 10^{-3} \text{ s}^{-1}$, pull-in failures limits stretch to small values. The trade-off situation is that high actuator output forces are obtained at low stretch rates, right in the pull-in failure

domain. Thus, for reliable operation at large extension, DEAs must operate at higher stretch rates at the cost of lower output forces.

Fig. 9b shows that between the two performance limits of pull-in failures and viscous impedance, dielectric strength is the dominant performance limiter. In this regime, large output stretches of at least 2.5 are possible.

Fig. 9c superpose actuator efficiency (taken from Fig. 6) over the possible stretch domain. The figure shows an arbitrary efficiency limit of 1% indicating how efficiency varies greatly inside the possible stretch domain. Low stretch rates and high extension conditions have poor efficiencies due to current leakage and are not suitable for applications where energy conservation is critical.

Fig. 9d shows the location of the performance metric peaks inside the possible stretch domain. For diamond actuators, peak force and peak power are pretty much stretch independent and are therefore shown as dotted regions. The best performance numbers are widely separated and cannot be obtained simultaneously. Design trade-offs are not only essential between actuator performance and reliability, but also between the performance metrics themselves. This makes the selection of actuator working conditions highly application dependant.

Fig. 9 identifies two important limitations of DEAs based on VHB 4905/4910: pull-in failure and current leakage. The consequence of these limitations on actuator design is significant. Actuators cannot be thought of as elastic films with minor viscous effects and negligible current leakage. These effects are dominant and must be accounted for in the design of practical actuators.

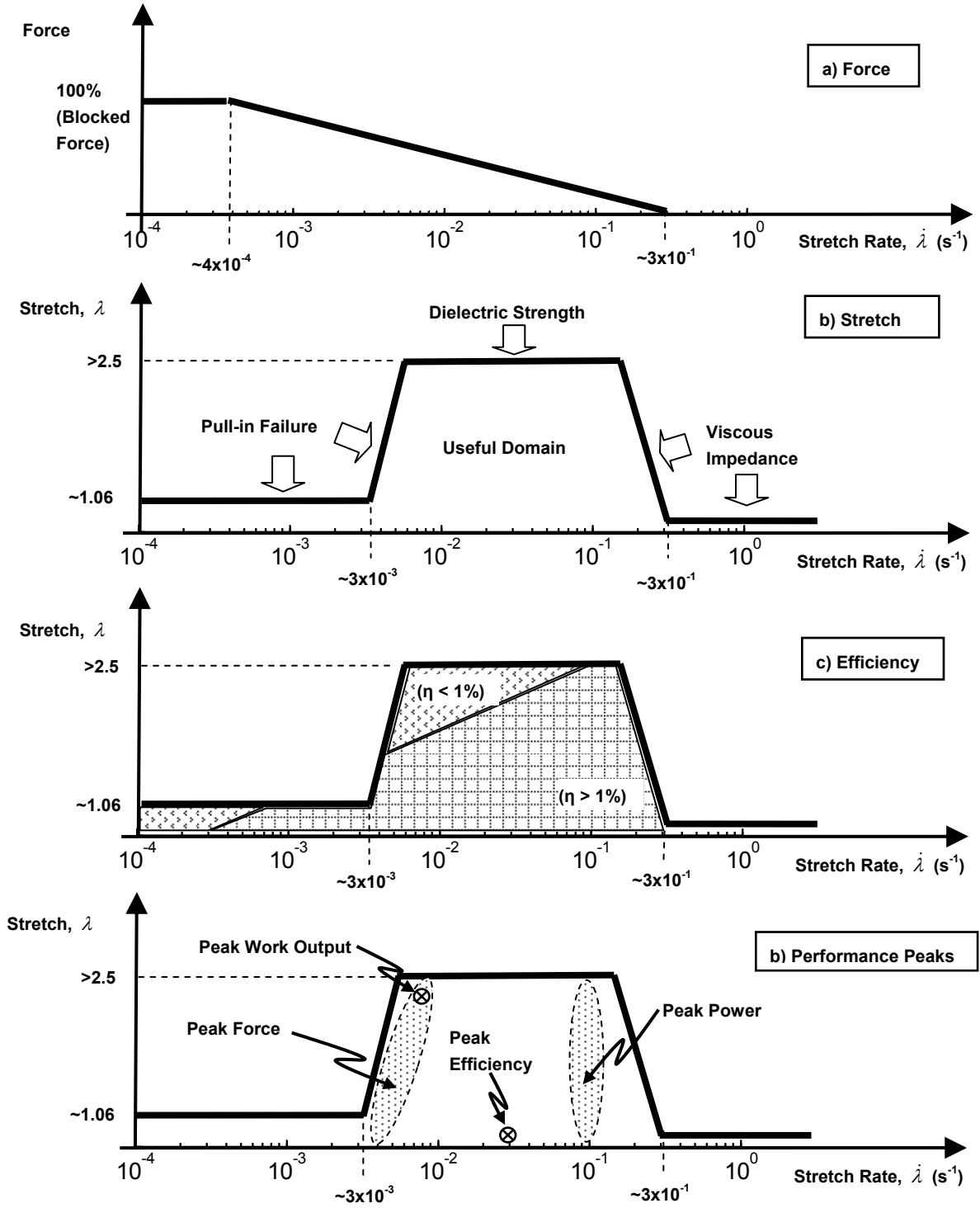


Fig. 9: Design space of DEAs based on VHB 4905/4910.

4.2. Possible Applications

As shown in Fig. 9, the principal performance limiter of DEA using VHB 4905/4910 are pull-in, current leakage, and viscous losses. Viscous losses limits force and extension at high speeds. Pull-in and current leakage prevent maintaining significant loads for long periods of time at high extensions. It should be noted that actuators operating under no load conditions are much less limited by pull-in provided that their films are sufficiently pre-stretched [27]. However, this paper focuses on practical actuators that are intended to do work on external systems and such unloaded cases are not considered. There are known robotics and mechatronics applications that fit inside the design space of Fig. 9. These are:

A) Low extensions:

Keeping the stretches below a safe threshold (here 1.06) can prevent pull-in failure and allow to maintain loads for any stretch rates. However, maintaining loads over long periods of time would likely cause low efficiencies due to current leakage. Depending on the application, low efficiencies might be tolerable. Applications like micro-valve actuation could enter this low extension category.

B) Alternating motion:

Any application where DEAs are cycled at sufficiently high stretch rates appears to be desirable. Applications like rotary motors [13,16], flapping wings mechanisms [13,16], and cardiac pumps [8,9] enters this category.

C) Bistable actuation:

Bistable actuation uses actuators intermittently at high stretch rates to switch the state of a bistable device [10,26]. Actuators are not powered during state holding and are allowed to return to their no-power configuration. Applications such as powered air vents traps in HVAC systems, automotive door locks, and binary robotics could use bistable actuators. Binary robotics is a concept of robotics where smooth and

continuous motion is approximated by using a large number of binary actuators, each having two states, extended or contract.

4.3. Comparison with Electromagnetic Actuators.

The properties of DEA identified in this paper are used to explain how they differ from the well established electromagnetic technology. Table 1 shows a performance comparison of a laboratory grade diamond actuator using 3 active film layers and a commercially available voice coil actuator (BEI Kimco Magnetic division, part number LA15-26-000A, see: <http://www.beikimco.com/>). The comparison is done with the best possible values measured to date. Care should be taken in using these numerical results because the DEA tested here is not an optimized device whereas electromagnetic actuators have been developed for more than a century with massive efforts.

Table 1: DEAs vs. electromagnetic [26].

Criteria	DEA	Voice Coils
Max. strains	150%	48%
Maintain large extensions under load	Poor	Good
Max. velocity	~ 5 mm/s	~ 5000 mm/s
Max. specific work output	0.003 J/g	0.006 J/g
Max. force-to-weight	13	13
Max. power-to-weight	0.0001 W/g	0.16 W/g
Max. efficiency	12%	80%

The following comparisons can be made based on Table 1:

- DEAs show higher strains than voice coils, provided they operate in their optimum working conditions where dielectric strength is the limiting factor.
- Voice coils are better to maintain loads at high extensions because they are limited by thermal dissipation whereas DEA are limited by pull-in instability.

- Voice coils can operate up to 1000 times faster because they are not subject to viscous impedance. Since, both technologies have similar specific work output and force-to-weight ratios, the significantly higher speeds of voice coils give them much higher power-to-weight ratios (Recall that $\text{Power} = \text{Force} \times \text{velocity}$).
- Voice coils are more efficient because DEAs show significant current leakage.

5. CONCLUSIONS

This paper presented the results of fundamental studies of DEAs based on diamond actuators and VHB 4905/4910 material conducted to understand how to design reliable, high performance actuators. In particular, four key mechanisms were discussed: pull-in failure, dielectric strength failure, viscoelasticity and current leakage.

Analytical model predictions compared with experimental data showed how stretch rate affects the failure modes of these DEAs. In particular, diamond actuators using VHB 4905/4910 and operating under load appear impractical for low speeds or continuous usage due to pull-in failure limitations. To be reliable, DEAs must operate at high stretch rates where they are most likely limited by the film's dielectric strength. An experimental performance characterization shows how viscoelasticity and current leakage affect performance. Viscous impedance reduces actuation forces (and extension) as speed increases. Large current leakage occurring at high extension and low speeds negatively affect efficiency.

A preliminary map of the design space of DEAs was proposed based on the fundamental properties identified in this paper. The map is for diamond actuators using VHB 4905/4910 and should represent the general trends of DEAs. Based on this design space, possible applications of DEAs have been proposed and major differences with well-known electromagnetic actuators were explained.

As new film materials are developed, DEA performance will surely improve. However, the four mechanisms discussed in this paper will remain important considerations in the design of DEAs.

ACKNOWLEDGMENT

This work was done with sponsorship of the Cambridge-MIT Institute (CMI), the Center for Integration of Medicine and Innovative Technology (CIMIT), and the NASA Institute for Advanced Concept (NIAC). The authors extend their thanks to Professors M. Boyce and R. Abeyaratne for the valuable discussions, and to Sam Korb for his contribution to experimental work.

REFERENCES

-
- ¹ Meijer K, Rosenthal M and Full R J 2001 Muscle-Like Actuators? A Comparison Between Three Electroactive Polymers *Smart Structures and Materials 2001: Electroactive Polymer Actuators and Devices* **4329** 7-15
 - ² Pelrine R, Kornbluh R, Joseph J and Chiba S 1997 Electrostriction of Polymer Films for Microactuators *Proceedings - IEEE Tenth Annual International Workshop on Micro Electro Mechanical Systems, Nagoya, Japan*, 238-243
 - ³ Kofod G, 2001 Dielectric Elastomer Actuators *Ph.D. Thesis, Department of Chemistry, The Technical University of Denmark, Denmark*
 - ⁴ Pei Q, Pelrine R, Rosenthal M, Stanford S, Prahlad H and Kornbluh R 2004 Recent Progress on ElectroElastomer Artificial Muscles and their Application for Biomimetic Robots *Smart Structures and Materials 2004: Electroactive Polymer Actuators and Devices* **5385** 41-50
 - ⁵ Vogan J, Wingert A, Hafez M, Plante JS, Dubowsky S, Kacher D and Jolesz F 2004 Manipulation in MRI Devices Using Electrostrictive Polymer Actuators: with an Application to Reconfigurable Imaging Coils *2004 IEEE International Conference on Robotics and Automation, New Orleans, Louisiana*, **2004** 2498-504
 - ⁶ Hanson D and V White 2004 Converging the Capabilities of EAP Artificial Muscles and the Requirements of Bio-Inspired Robotics *Smart Structures and Materials 2004: Electroactive Polymer Actuators and Devices* **5385** 29-40
 - ⁷ Kornbluh R, Pelrine R, Prahlad H and Heydt R 2004 Electroactive Polymers: An Emerging Technology for MEMS *MEMS/MOEMS Components and Their Applications 2004, San Jose, CA* **5344** 13-27
 - ⁸ Goulbourne N, Frecker M, Mockensturm E and Snyder A 2003 Modeling of a Dielectric Elastomer Diaphragm for a Prosthetic Blood Pump *Smart Structures and Materials 2003: Electroactive Polymer Actuators and Devices* **5051** 319-31
 - ⁹ Goulbourne N, Frecker M and Mockensturm E 2004 Electro-Elastic Modeling of a Dielectric Elastomer Diaphragm for a Prosthetic Blood Pump *Smart Structures and Materials 2004: Electroactive Polymer Actuators and Devices* **5385** 122-33
 - ¹⁰ Vogan J 2004 Development of Dielectric Elastomer Actuators for MRI Devices, *M.S. Thesis, Department of Mechanical Engineering, Massachusetts Institute of Technology, Cambridge, MA*
 - ¹¹ Wingert A 2002 Development of a Polymer-Actuated Binary Manipulator, *M.S. Thesis, Department of Mechanical Engineering, Massachusetts Institute of Technology, Cambridge, MA*
 - ¹² Carpi F, Migliore A and De Rossi D 2005 A New Contractile Linear Actuator Made of Dielectric Elastomers *Smart Structures and Materials 2005: Electroactive Polymer Actuators and Devices* **5759** 64-74
 - ¹³ Kornbluh R, Pelrine R, Pei Q, Heydt R, Stanford S, Oh S and Eckerle J 2002 Electroelastomers: Applications of Dielectric Elastomer Transducers for Actuation, Generation and Smart Structures *Smart Structures and Materials 2002: Electroactive Polymer Actuators and Devices* **4695** 254-70
 - ¹⁴ Pei Q, Rosenthal M, Pelrine R, Stanford S and Kornbluh R 2003 Multifunctional Electroelastomer Roll Actuators and Their Application for Biomimetic Walking Robots *Smart Structures and Materials 2003: Electroactive Polymer Actuators and Devices* **5051** 41-50
 - ¹⁵ Pelrine R, Kornbluh R, Pei Q, Stanford S, Oh S and Eckerle J 2002 Dielectric Elastomer Artificial Muscle Actuators: Toward Biomimetic Motion *Smart Structures and Materials 2002: Electroactive Polymer Actuators and Devices* **4695** 126-37
 - ¹⁶ Pelrine R, Sommer-Larsen P, Kornbluh R, Heydt R, Kofod G, Pei Q and Gravesen P 2001 Applications of Dielectric Elastomer Actuators *Smart Structures and Materials 2001: Electroactive Polymer Actuators and Devices* **4329** 335-49
 - ¹⁷ Schlaak H F, Jungmann M, Matysek M and Lotz P 2005 Novel Multilayer Electrostatic Solid-State Actuators with Elastic Dielectric *Smart Structures and Materials 2005: Electroactive Polymer Actuators and Devices* **5759** 121-33
 - ¹⁸ Kornbluh R, Pelrine R, Joseph J, Heydt R, Pei Q and Chiba S 1999 High-Field Electrostriction of Elastomeric Polymer Dielectrics for Actuation *Smart Structures and Materials: Electro-Active Polymer Actuators and Devices* **3669** 149-61
 - ¹⁹ Pelrine R, Kornbluh R and Joseph J 1998 Electrostriction of Polymer Dielectrics with Compliant Electrodes as Means of Actuations *Sensor and Actuators A: Physical* **64** 77-85

-
- ²⁰ Sommer-Larsen P, Hooker J, Kofod G, West K, Benslimane M and Gravesen P 2001 Response of Dielectric Elastomer Actuators *Smart Structures and Materials 2001: Electroactive Polymer Actuators and Devices* **4329** 157-63
- ²¹ Kornbluh R, Pelrine R, Pei Q, Oh S and Joseph J 2000 Ultrahigh Strain Response of Field-Actuated Elastomeric Polymers *Smart Structures and Materials 2000: Electroactive Polymer Actuators and Devices* **3987** 51-64
- ²² Ma W, and Cross L E 2004 An Experimental Investigation of Electromechanical Response in a Dielectric Acrylic Elastomer *Applied Physics - Materials Science & Processing A* **78** 1201-4
- ²³ Larsen P, Kofod G, Benslimane M, Gravesen P, and Shridhar M H 2002 Performance of Dielectric Elastomer Actuators and Materials *Smart Structures and Materials 2002: Electroactive Polymer Actuators and Devices* **4695** 158-66
- ²⁴ Wissler M, and Mazza E 2005 "Modeling of a Pre-Strained Circular Actuator Made of Dielectric Elastomers *Sensors and Actuators* **120** 184-92
- ²⁵ Yang E, Frecker M, and Morckensturm E 2005 Viscoelastic Model of Dielectric Elastomer Membranes *Smart Structures and Materials 2005: Electroactive Polymer Actuators and Devices, San Diego CA* **5759** 82-93
- ²⁶ Plante JS 2006 Dielectric Elastomer Actuators for Binary Robotics and Mechatronics *Ph.D. Thesis Department of Mechanical Engineering, Massachusetts Institute of Technology, Cambridge, MA*
- ²⁷ Plante JS, and Dubowsky S 2006 Large Scale Failure Modes of Dielectric Elastomer Actuators *in press: International Journal of Solids and Structures*
- ²⁸ Plante JS and Dubowsky S 2006 Performance Mechanisms of Dielectric Elastomer Actuators *Journal paper in preparation*
- ²⁹ Holzapfel G A 2000 Nonlinear Solid Mechanics *Chichester, UK: John Wiley & Sons*
- ³⁰ Ogden R W 1984 Non-Linear Elastic Deformations *New York: Dover Publications*
- ³¹ Cameron C, Underhill R, Rawji M, and Szabo J 2004 Conductive Filler – Elastomer Composites for Maxwell Stress Actuator Applications *Smart Structures and Materials 2004: Electroactive Polymer Actuators and Devices* **5385** 51-9
- ³² Carpi F, Mazzoldi A and De Rossi D 2003 High-Strain Dielectric Elastomer for Actuation *Smart Structures and Materials 2003: Electroactive Polymer Actuators and Devices* **5051** 419-22
- ³³ Kornbluh R, Pelrine R, Pei Q, Oh S and Joseph J 2000 Ultrahigh Strain Response of Field-Actuated Elastomeric Polymers *Smart Structures and Materials 2000: Electroactive Polymer Actuators and Devices* **3987** 51-64
- ³⁴ Kornbluh R, Pelrine R and Joseph J 1995 Elastomeric Dielectric Artificial Muscle Actuators for Small Robots *Proceedings of the Materials Research Society Symposium* **600** 119-30
- ³⁵ Ladeggard Larsen A, Sommer-Larsen P and Hassager O 2004 How to Tune Rubber Elasticity *Smart Structures and Materials 2004: Electroactive Polymer Actuators and Devices* **5385** 108-117
- ³⁶ Pelrine R, Kornbluh R, Joseph J and Chiba S 1997 Electrostriction of Polymer Films for Microactuators *Proceedings - IEEE Tenth Annual International Workshop on Micro Electro Mechanical System* 238-243
- ³⁷ Sommer-Larsen P and Ladeggard Larsen A 2004 Materials for Dielectric Elastomer Actuators *Smart Structures and Materials 2004: Electroactive Polymer Actuators and Devices* **5385** 68-77
- ³⁸ Szabo J, Hiltz J, Cameron C, Underhill R, Massey J, White B, and Leidner J 2003 Elastomeric Composites with High Dielectric Constant for use in Maxwell Stress Actuators *Smart Structures and Materials 2003: Electroactive Polymer Actuators and Devices* **5051** 180-90
- ³⁹ Zhang X, Wissler M, Jaehne B, Broennimann R and Kovacs G 2004 Effects of Crosslinking, Prestrain and Dielectric filler on the Electromechanical Response of a New Silicone and Comparison with Acrylic Elastomer *Smart Structures and Materials 2004: Electroactive Polymer Actuators and Devices* **5385** 78-86
- ⁴⁰ Kofod G, Kornbluh R, Pelrine R and Sommer-Larsen P 2001 Actuation Response of Polyacrylate Dielectric Elastomers *Smart Structures and Materials 2001: Electroactive Polymer Actuators and Devices* **4329** 141-7
- ⁴¹ Ritchie P D 1965 Physics of Plastics *Princeton, N.J: Van Nostrand*